*Inorg. Chem.* **2008**, *47*, 9763−9765

Inorganic Chemistry
Communication

# Ferromagnetic Dy−Ni and Antiferromagnetic Dy−Cu Couplings in Single-Molecule Magnets [$Dy_2Ni$] and [$Dy_2Cu$]

**Atsushi Okazawa,[†] Takashi Nogami,[†] Hiroyuki Nojiri,[‡] and Takayuki Ishida*,[†]**

*Department of Applied Physics and Chemistry, The University of Electro-Communications, Chofu, Tokyo 182-8585, Japan, and Institute for Materials Research, Tohoku University, Katahira, Sendai 980-8577, Japan*

Received September 2, 2008

The exchange couplings in [{Dy(hfac)$_3$}$_2$Cu(dpk)$_2$] and [{Dy(hfac)$_3$}$_2$-Ni(dpk)$_2$(py)$_2$] (Hdpk = di-2-pyridyl ketoxime) were precisely evaluated by high-frequency electron paramagnetic resonance and pulsed-field magnetization studies, giving $J_{Dy-Cu}/k_B = -0.126$ K and $J_{Dy-Ni}/k_B = +0.031$ K.

Single-molecular magnets (SMMs) exhibit magnetic hysteresis from the single-molecular origin,[1] namely, extremely slow magnetization reversal due to a high energy barrier. Lanthanide ions seem suitable for the development of SMMs because the barrier is caused by strong magnetic anisotropy and large spins.[2] Our idea was that 4f−3d heterometallic compounds would have larger spins whichever ferro- or antiferromagnetic coupling is operative between 4f and 3d spins. Actually, several Dy−Cu compounds showed slow magnetization reversal and distinct hysteresis, as clarified by alternating current (ac) susceptibility and pulsed-field magnetization measurements.[3−8] Quantum tunneling of magnetization (QTM), observable as magnetization steps, is also characteristic of SMMs.[1] In the present work, we investigated the exchange couplings and energy-level structures of linear trinuclear 4f−3d-heterometallic compounds by means of high-frequency electron paramagnetic resonance (HF-EPR)[9] together with pulsed-field magnetization.[10] A number of 4f−3d heterometallic SMMs are known to date,[3−8] but the magnitude of intramolecular exchange coupling has rarely been determined so far.[3−5] We have established a standard method to evaluate the exchange couplings.

**Chart 1.** Structural Formulas of [$Dy_2Cu$] and [$Dy_2Ni$]

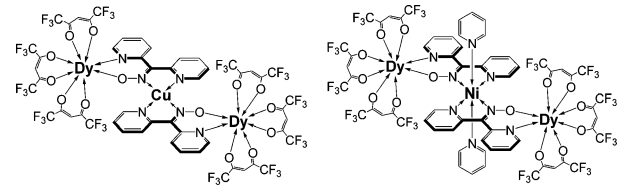


Complexes [{$Dy^{III}$(hfac)$_3$}$_2$$Cu^{II}$(dpk)$_2$][3] and [{$Dy^{III}$(hfac)$_3$}$_2$-$Ni^{II}$(dpk)$_2$(py)$_2$][11] (abbreviated as [$Dy_2Cu$] and [$Dy_2Ni$], respectively) were prepared according to the literature method (Hhfac = 1,1,1,5,5,5-hexafluoropentane-2,4-dione; Hdpk = di-2-pyridyl ketoxime; for the molecular structures, see Chart 1). They crystallized in a monoclinic $P2_1/n$ space group. The molecular structures are similar to each other except for the additional axial pyridine ligands in [$Dy_2Ni$]. There is a unique $J_{4f-3d}$ exchange parameter in each compound, owing to a molecular centrosymmetry.

The pulse-field magnetization measurements on a polycrystalline specimen of [$Dy_2Ni$] clarified hysteresis behavior with magnetization jumps (Figure 1). The positions of the jumps indicated by the peaks of the differential magnetization show no appreciable field-sweeping rate or temperature dependence, being compatible with the QTM. The slow magnetization reversal has already been demonstrated from ac magnetic susceptibility.[11,12] Combining the results on [$Dy_2Cu$] previously reported,[3] we can conclude that [$Dy_2Cu$] and [$Dy_2Ni$] are isomorphous SMMs. Evaluation of $J_{4f-3d}$ and of the energy level for each compound is now the next problem, which seems difficult to solve solely from magnetization studies.

HF-EPR spectra of powder [$Dy_2Cu$] were collected in a wide frequency range between 41.2 and 190 GHz at 4.2 K (Figure

* To whom correspondence should be addressed. E-mail: ishi@pc.uec.ac.jp.
[†] The University of Electro-Communications.
[‡] Tohoku University.

(1) (a) Gatteschi, D.; Sessoli, R.; Villain, J. *Molecular Nanomagnets*; Oxford University Press: New York, 2006. (b) Gatteschi, D.; Sessoli, R. *Angew. Chem., Int. Ed.* **2003**, *42*, 268.
(2) (a) Ishikawa, N.; Sugita, M.; Ishikawa, T.; Koshihara, S.-y.; Kaizu, Y. *J. Am. Chem. Soc.* **2003**, *125*, 8694. (b) Ishikawa, N.; Sugita, M.; Wernsdorfer, W. *J. Am. Chem. Soc.* **2005**, *127*, 3650.
(3) Mori, F.; Nyui, T.; Ishida, T.; Nogami, T.; Choi, K.-Y.; Nojiri, H. *J. Am. Chem. Soc.* **2006**, *128*, 1440.
(4) Ueki, S.; Ishida, T.; Nogami, T.; Choi, K.-Y.; Nojiri, H. *Chem. Phys. Lett.* **2007**, *440*, 263.
(5) Okazawa, A.; Nogami, T.; Nojiri, H.; Ishida, T. *Chem. Mater.* **2008**, *20*, 3110.
(6) Osa, S.; Kido, T.; Matsumoto, N.; Re, N.; Pochaba, A.; Mrozinski, J. *J. Am. Chem. Soc.* **2004**, *126*, 420.
(7) Aronica, C.; Pilet, G.; Chastanet, G.; Wernsdorfer, W.; Jacquot, J. F.; Luneau, D. *Angew. Chem., Int. Ed.* **2006**, *45*, 4659.
(8) Costes, J. P.; Shova, S.; Wernsdorfer, W. *Dalton Trans.* **2008**, 1843.
(9) Nojiri, H.; Choi, K.-Y.; Kitamura, N. *J. Magn. Magn. Mater.* **2007**, *310*, 1468.
(10) Nojiri, H.; Ajiro, Y.; Asano, T.; Boucher, J.-P. *New J. Phys.* **2006**, *8*, 218.
(11) Mori, F.; Ishida, T.; Nogami, T. *Polyhedron* **2005**, *24*, 2588.
(12) Preliminary Arrhenius analysis on [$Dy_2Ni$] gave $T_B = 2.5$ K, $E_a/k_B = 66$ K, and $\tau_0 = 1.0 \times 10^{-7}$ s.

10.1021/ic801686z CCC: $40.75 
Published on Web 10/10/2008

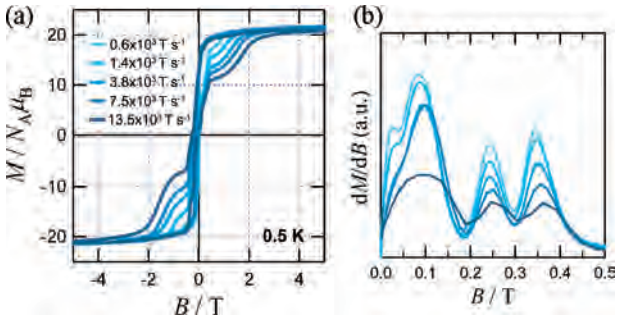


**Figure 1.** (a) Hysteresis curves for [$Dy_2Ni$] measured at 0.5 K. The field-sweeping rates were (0.6−13.5) × $10^3$ T $s^{-1}$. (b) Differential magnetization curves as a function of the sweeping rate.

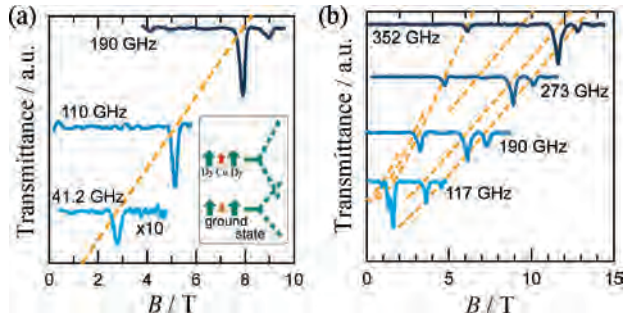


**Figure 2.** Selected EPR spectra measured at 4.2 K as a function of the frequency for (a) [$Dy_2Cu$] and (b) [$Dy_2Ni$]. The spectra are offset in a linear scale of the frequency. Dotted lines are drawn as a guide to the eye. The inset in part a schematically shows two related states of [$Dy_2Cu$] near zero field.

2a). We found a series of major signals shifted to a higher field with an increase of the frequency. The $g$ value was 2.07(1) from the slope of the frequency-field plot, being consistent with the Cu signal satisfying a conventional EPR selection rule of $\Delta m_s = \pm 1$. There is no single-ion-type anisotropy in Cu spins, and thus the observed characteristic frequency-field relation shows the presence of internal fields on the Cu sites mediated by sizable exchange couplings between Dy and Cu ions. In other words, the observed EPR is attributed to the reversal of the Cu $S = {}^1/_2$ spin biased by the exchange field from the Dy ions. Extrapolation gives a critical field of 1.36 T. It is identical with the position of a 2-$\mu_B$ jump due to the Cu spin flip in the magnetization curves.[3]

The temperature dependence of the EPR signal intensity indicates that this absorption band was ascribable to the transition from the ground state. Owing to the level cross at 1.36 T, the ferromagnetic state [Dy(↑)−Cu(↑)−Dy(↑)] becomes the lowest in this region, and excitation to a ferrimagnetic state [Dy(↑)−Cu(↓)−Dy(↑)] was observed. The ground state of [$Dy_2Cu$] at zero field is ferrimagnetic (the inset of Figure 2a).

By treatment of the Dy moments as Ising spins with $|J^z| = {}^{15}/_2$ and $g_{Dy} = {}^4/_3$, an Ising-type spin Hamiltonian (eq 1) can be built as an exchange coupling model here.[3] The first term implies exchange interaction and the second the Zeeman effect. There is a single adjustable parameter $J_{Dy-Cu}$, and accordingly $J_{Dy-Cu}/k_B$ can be easily determined to be −0.126(3) K by fitting the EPR result. This value is close to that from the magnetization study (−0.155 K),[3] but the present value has a much better

(13) Rebilly, J.-N.; Charron, G.; Riviere, E.; Guillot, R.; Barra, A.-L.; Serrano, M. D.; van Slageren, J.; Mallah, T. *Chem.—Eur. J.* **2008**, *14*, 1169.

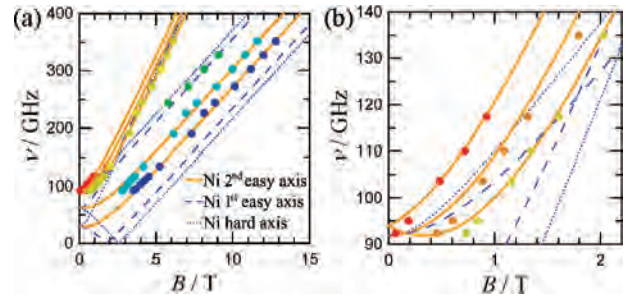


**Figure 3.** Frequency-field diagrams for (a) [$Dy_2Ni$] and (b) its magnification in a small magnetic field region. Circles: data. Lines: calculation from the energy-level diagram (Figure 4).

precision because of the high resolution of HF-EPR and the variable-frequency technique. We note here that the exchange energy is as large as 0.47 K because of the long Dy moment.

$$\hat{H} = -J_{Dy-Cu}(\hat{J}^z_{Dy1}\cdot\hat{S}_{Cu} + \hat{J}^z_{Dy2}\cdot\hat{S}_{Cu}) + \mu_B H^z(g_{Dy}J^z_{Dy1} + g_{Dy}J^z_{Dy2} + g_{Cu}S_{Cu}) \quad (1)$$

HF-EPR spectra of powder [$Dy_2Ni$] were recorded in a frequency range of 92.4−352 GHz at 4.2 K (Figure 2b). We found three "allowed" $g \approx 2$ lines and three "forbidden" $g \approx 4$ lines. This finding indicates that the local symmetry of the $Ni^{2+}$ single-ion-type anisotropy is orthorhombic with zero-field-splitting (ZFS) $D$ and $E$ terms. No Dy signal was observed like in the [$Dy_2Cu$] case.

The EPR frequency-field relations of $Ni^{2+}$ compounds with orthorhombic symmetry are well-known,[13] and Figure 2b demonstrates a typical transverse-field pattern for Ni ions. Two intense bands out of three $g \approx 2$ lines are ascribable to absorption bands for the Ni second easy axis. The other minor band is assigned to that for the first. The powder sample was loosely packed, and each microcrystal underwent reorientation to the easy axis in a sample room. If the easy axes of Dy and Ni were close to each other, the sample could be oriented along those axes. Then Ni EPR spectra of the easy axis would be expected, which is different from the present result. Therefore, the easy-axis directions of Ni and Dy are different from each other, and the sample powder is reoriented so that the Dy moments align along the field direction. As a result, the Ni spin experiences a transverse field.

Though the spectra are somewhat complex in comparison with those of [$Dy_2Cu$], the basic concept holds for [$Dy_2Ni$]. We extend the Ising model as follows (eq 2).

$$\hat{H} = -J_{Dy-Ni}(\hat{J}^z_{Dy1}\cdot\hat{S}^z_{Ni} + \hat{J}^z_{Dy2}\cdot\hat{S}^z_{Ni}) + D_{Ni}\left(\hat{S}^{z\,2}_{Ni} - \frac{1}{3}S_{Ni}(S_{Ni}+1)\right) + E_{Ni}(\hat{S}^{x\,2}_{Ni} - \hat{S}^{y\,2}_{Ni}) + \mu_B H^z(g_{Dy}J^z_{Dy1} + g_{Dy}J^z_{Dy2}) + \mu_B g_{Ni}S_{Ni}\cdot H \quad (2)$$

where $J_{Dy-Ni}$ is an exchange coupling. The ZFS terms defined by $D_{Ni}$ and $E_{Ni}$ are incorporated in eq 2. The last term implies the Zeeman effect on the Heisenberg Ni spin. The coordinate is defined as $z$ along the Dy easy axis and $y$ along the Ni first easy axis. The fitting result is given in Figure 3.

The forbidden line is usually single, but there were three $g \approx 4$ lines in the present study. This finding can be plausibly interpreted only when the sublevels due to the Dy−Ni exchange interaction are taken into consideration in addition to the usual

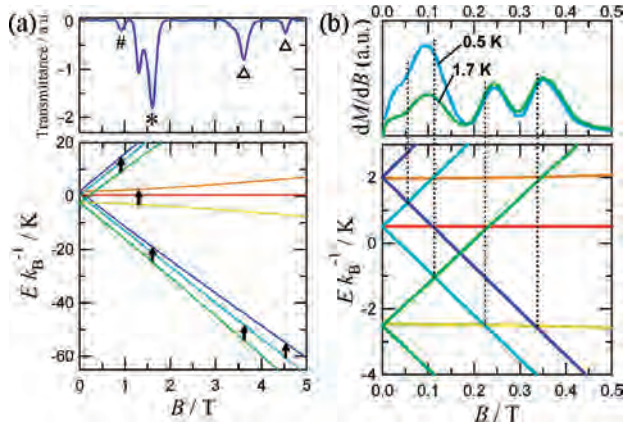


**Figure 4.** Schematic Zeeman diagrams of (a) $[Dy_2Ni]$ and (b) its magnification in a small magnetic field region. The EPR absorption spectrum at 117.4 GHz and 4.2 K is also shown in the top of part a. The differential magnetization curves measured at 0.5 and 1.7 K with a field-sweeping rate of $3.6 \times 10^3$ T $s^{-1}$ are also shown in the top of part b.

ZFS. For simplicity, the exchange term is replaced by the exchange bias field in the fitting. Finally, we obtained $J_{Dy-Ni}/k_B = +0.031$ K, $D_{Ni}/k_B = +3.7$ K, and $E_{Ni}/k_B = -0.73$ K with $g_{Ni} = 2.10$. Though $J_{Dy-Ni}$ is small, the fitting was impossible without this coupling. The sign of the exchange coupling is opposite to that of Dy−Cu. The Dy and Ni spins are ferromagnetically coupled.

The sign of $D_{Ni}$ was determined from the intensity ratio of the allowed bands (denoted with Δ in Figure 4a). The ground state was confirmed by the variable-temperature experiments. Such a technique has been widely applied to the determination of $D$ values in 3d-based SMMs.[14]Note that the present application of HF-EPR to evaluate the exchange coupling is quite unique. The profile of the forbidden bands is sensitive to the sign of $J_{Dy-Ni}$. The Ni forbidden band due to excitation from Dy(↑)−Ni(↑)−Dy(↑) to Dy(↑)−Ni(↓)−Dy(↑) (denoted as * in Figure 4a) is the strongest because of a transition from the ground state. On the other hand, the band from Dy(↓)−Ni(↑)−Dy(↓) to Dy(↓)−Ni(↓)−Dy(↓) is the weakest (# in Figure 4a) because this transition takes place between higher-energy states. The stronger band appears in the higher field when $J_{Dy-Ni}$ is positive. If $J_{Dy-Ni}$ were negative, the stronger band would appear in the lower field. We confirmed this by simulation works.

The above description with arrows is valid only in very high fields. The Dy and Ni spins are ferromagnetically coupled, and at the same time, the Ni single-ion anisotropy directs the Ni spin perpendicular to the $z$ axis [i.e., Dy(↑)−Ni(→)−Dy(↑)]. Consequently, the Ni spin is tilted from the $z$ axis at the ground state in zero field. The magnitude of tilting is regulated by the balance between the exchange coupling and the Ni single-ion anisotropy.


**Figure 5.** Coordination structures of (a) $DyO_7N$ and $CuN_4$ in $[Dy_2Cu]$ and (b) $DyO_7N$ and $NiN_6$ in $[Dy_2Ni]$. Planes stand for the Dy basal plane of a square antiprism (orange) and the Cu or Ni equatorial plane (blue).

The pulsed-field magnetization data supported the antiferro- and ferromagnetic couplings in $[Dy_2Cu]$ and $[Dy_2Ni]$, respectively. While a 2-$\mu_B$ jump due to the spin flip of the Cu spin was observed for the former,[3] the corresponding 4-$\mu_B$ jump due to the Ni spin was missing for the latter (Figure 1), even when the field was swept up to a very high magnetic field of 18 T. This indicates that $J_{Dy-Ni}$ is ferromagnetic. The present $[Dy_2Ni]$ energy-level structure completely agrees with the EPR signal positions, taking the 117.4 GHz data, for example, in Figure 4a. As for several level crossings in a small field region (Figure 4b), they clearly coincide with the positions of the magnetization jumps. Thus, the present model is totally consistent with both the magnetization and EPR results.

There are ample reports on ferromagnetic $J_{Dy-Cu}$ as well as $J_{Gd-Cu}$.[15−17] Antiferromagnetic couplings are explained in terms of the violation of the ferromagnetic interaction between the 4f spin portion and the 3d spin,[15] owing to torsion along the Ln(4f)−O−N−M(3d) linkage.[18] The presence of the Ni axial ligands seems responsible for the geometrical modification. As shown in Figure 5, the basal plane of the $DyO_7N$ square antiprism is almost parallel to the $CuN_4$ square plane. On the other hand, a dihedral angle between the corresponding planes in $[Dy_2Ni]$ is considerably larger (ca. 20°) because of the steric repulsion between pyridine and $CF_3$ groups. The Dy−O−N−M torsions largely differ from each other: 117.8(5)° for $[Dy_2Cu]$ versus 143.7(5)° for $[Dy_2Ni]$. The smaller out-of-plane distortion in the latter favors ferromagnetic coupling.

The advantages of HF-EPR are its extremely high resolution and its ability to identify quantum numbers of energy levels by the EPR selection rule. In the present work, the Dy signal itself was unobservable, but the bias field at the 3d metal ions was detected, affording information of exchange couplings. The magnitude of $J_{4f-3d}$ has rarely been determined for 4f−3d SMMs.[5] We have precisely evaluated $J_{4f-3d}$ and depicted energy levels for $[Dy_2Cu]$ and $[Dy_2Ni]$. The present methodology would be applicable to other 4f−3d heterometallic SMM compounds.

**Acknowledgment.** This work was partly supported by Grants-in-Aid for Scientific Research from MEXT, Japan, and the Inter-University Cooperative Research Program of IMR, Tohoku University. A part of this work was performed at CINTS, Tohoku University.

IC801686Z

(14) Barra, A. L.; Gatteschi, D.; Sessoli, R. *Phys. Rev. B* **1997**, *56*, 8192. Bouwen, A.; Caneschi, A.; Gatteschi, D.; Goovaerts, E.; Schoemaker, D.; Sorace, L.; Stefan, M. *J. Phys. Chem. B* **2001**, *105*, 2658.

(15) Andruh, M.; Ramade, I.; Codjovi, E.; Guillou, O.; Kahn, O.; Trombe, J. C. *J. Am. Chem. Soc.* **1993**, *115*, 1822.

(16) (a) Costes, J. P.; Dahan, F.; Dupuis, A. *Inorg. Chem.* **2000**, *39*, 5994. (b) Costes, J. P.; Dahan, F.; Dupuis, A.; Laurent, J. P. *Inorg. Chem.* **2000**, *39*, 169. (c) Costes, J.-P.; Dahan, F.; Dupuis, A.; Laurent, J.-P. *Chem.—Eur. J.* **1998**, *4*, 1616.

(17) (a) Kido, T.; Ikuta, Y.; Sunatsuki, Y.; Ogawa, Y.; Matsumoto, N.; Re, N. *Inorg. Chem.* **2003**, *42*, 398. (b) Evangelisti, M.; Kahn, M. L.; Bartolome, J.; de Jongh, L. J.; Meyers, C.; Leandri, J.; Leroyer, Y.; Mathoniere, C. *Phys. Rev. B* **2003**, *68*, 184405.

(18) (a) Kobayashi, Y.; Ueki, S.; Ishida, T.; Nogami, T. *Chem. Phys. Lett.* **2003**, *378*, 337. (b) Ueki, S.; Kobayashi, Y.; Ishida, T.; Nogami, T. *Chem. Commun.* **2005**, 5223.